Epitaxial growth of two-dimensional Pb and Sn films on Al(111)

J. Yuhara* and Y. Shichida
Department of Materials, Physics and Energy Engineering,
Nagoya University, Furo-cho, Chikusa-ku, Nagoya 464-8603, Japan

ABSTRACT

Single and binary two-dimensional (2D) films of Pb and Sn on Al(111) at room temperature were investigated using low-energy electron diffraction (LEED) and scanning tunneling microscopy. The 2D Pb and Sn films form a (√31×√31)-Pb structure with close-packed six-fold symmetry and a ("2"×√3)-Sn structure with square-like fourfold symmetry, respectively. The 2D bimetallic Pb-Sn films only exhibit (√31×√31)-Pb and/or ("2"×√3)-Sn LEED patterns in any compositional ratio of Pb to Sn. Sub-monolayer Sn deposition on the 2D Pb film reveals ("2"×√3)-Sn LEED pattern, indicating the preferential formation of the 2D Sn film. These results indicate that monolayer Pb and Sn films are immiscible on Al(111).

Corresponding author: J. Yuhara
j-yuhara@nagoya-u.jp

I. Introduction

The fundamental understanding of two-dimensional (2D) metal prepared on a solid surface is important not only for purely scientific interest but also for technological applications. In a step towards post-graphene materials, silicene, germanene, and stanene have been predicted and synthesized as elemental 2D analogues of graphene [1-4]. Therefore, it is very interesting to study the epitaxial growth on other metal surfaces. So far, it has been reported by the present group that Sn monolayer films form a square-like structure on Rh(111) and Ru(0001) at room temperature deposition [5,6], while Pb monolayer films form a hexagonal close-packed 2D structure on Rh(111), Ru(0001), Ag(111), Cu(111), and Ni(111) [5-9].

On the other hand, immiscible Pb and Sn atoms form a 2D ordered alloy on Rh(111), while immiscible Pb and Bi atoms form a 2D solid solution alloy on Rh(111) [5,10]. The different structural properties of the 2D alloys may be explained by the Hume-Rothery rule that a solid solution will be formed when two elements have identical crystal structures and the relative difference in their atomic sizes is less than 15 % [11]. Pb and Bi monolayer films form a close-packed structure on Rh(111), while Sn monolayer film forms a square-like structure on Rh(111) [5,12]. The Bi atomic size for 2D film is 0.36 nm, which is only 6 % larger than the Pb atomic size [5,10]. Therefore, 2D Pb-Bi films form an all-proportional solid solution with a hexagonal close-packed structure [10]. On the other hand, The Sn atomic size for 2D film is 10 % smaller than the Pb atomic size [5,6,13]. It has been shown that the Pb and Sn atoms form an ordered alloy and a solid solution alloy depending on the surfaces [5,6,13]. Therefore, the structural properties of bimetallic monolayer films seem to be related to the supported surface properties.

In the present paper, we report the epitaxial growth of 2D Pb and Sn films on Al(111) at room temperature. Scanning tunneling microscopy (STM), low-energy electron diffraction (LEED), and Auger electron spectroscopy (AES) were used to examine the surface morphology, periodicity of the 2D film, and the surface concentration, respectively.

II. Experimental

The experiments were performed in an ultrahigh vacuum (UHV) chamber operating at base pressures of less than 5×10^{-10} mbar in the sample preparation chamber and in the analysis chamber. The system was equipped with a rear view LEED system and a UHV STM system (Omicron STM-1). Four-grid optics enabled Auger analysis in a retarding field. All STM images were acquired with tungsten tips in the constant current mode with a positive sample bias voltage at room temperature.

To prepare a clean Al(111) surface, the crystal was sputtered by 2-keV Ar^+ ions at room temperature and annealed at 550 °C. The sample was annealed by electron bombardment at a voltage of 650 V from a thoriated tungsten filament placed behind the sample plate. The temperatures were monitored by a type K thermocouple mounted on the tantalum clip of the sample holder. The cleanliness of the Al(111) surface was verified using AES and LEED; no contamination was detected with AES, and a distinct (1×1) LEED pattern was observed.

Pb and Sn were deposited onto the clean Al(111) surface at room temperature from a boron nitride crucible. The deposition rate was 0.2 monolayer (ML)/min, which was measured via a quartz crystal microbalance that was later calibrated with a Rutherford backscattering spectroscopy measurement [14]. We define 1 ML as an overlayer with the atomic density of an Al(111) layer: 1.22×10^{15} atoms/cm^2). Complete atomic layer of

Pb and Sn films on Al(111) were obtained at coverage of approximately 0.7 ML, so that we studied the total coverage of Pb and Sn up to 0.8 ML to investigate the 2D bimetallic films. Then, in order to confirm the immiscibility of Pb and Sn, Sn atoms are deposited on monolayer Pb film or vice versa. At each film for single and binary system, the amount of Pb and/or Sn is confirmed by AES and the surface is characterized by STM and LEED techniques.

III. Results and Discussion

Fig. 1(a) and 1(b) shows a typical STM image and LEED pattern of monolayer Pb films on Al(111). The STM image exhibits the layer-by-layer growth mode. Locally, three-dimensional (3D) islands are also observed. The LEED pattern shows the primitive spots from Al(111) as well as hexagonal close-packed Pb film. The primitive cells of Pb film and Ag(111) are shown as yellow and red lines, respectively, in Fig. 1(b). The atomic row direction for Pb film is rotated 19° from that for Al(111). The interatomic distance of Pb atoms is estimated to be 0.35 nm.

Fig. 2(a) shows the Pb atomic arrangement on Al(111) and the primitive cell of Pb film and the unit cell of Pb/Al(111), which corresponds to $(\sqrt{31}\times\sqrt{31})R8.95°$, are shown as yellow solid and white dotted lines, respectively. From the primitive spots of Pb film, atomic row is rotated for 19.9° clockwise from Al(111) atomic row and the interatomic distance is calculated to be 0.35 nm, which is very much similar to the interatomic distance in bulk. This result is consistent with the previous report by Th. Deniozou et al. that Pb overlayer forms a hexagonal unit cell whose side length is 0.35nm [15]. To date, it has been shown that Pb atoms form a hexagonal close-packed 2D structure on Rh(111), Ru(0001), Ag(111), Cu(111), Ni(111), and Pt(111) [7-11]. Typical Pb atomic arrangements are displayed in Figs. 2(b) and 2(c) for the case of Rh(111) and Ru(0001).

The Pb atoms have a tendency to form a hexagonal close-packed 2D structure, regardless of the interatomic distance of the substrate by rotating the Pb film to accommodate the substrate periodicity. As a result, the Pb interatomic distance is consistently 0.35 ± 0.01 nm on these surfaces.

Fig. 3(a) and 3(b) shows a typical STM image and LEED pattern of monolayer Sn films on Al(111). From the STM image, it is shown that Sn atoms do not form any 3D) islands at monolayer's coverage. STM images do not exhibit any 2D and 3D islands at submonlayer coverages in the case of Sn/Al(111), not like Sn/Rh(111) and Sn/Ru(0001) [5,6]. These results indicate that the Sn atoms are very mobile on Al(111) at room temperature. The high-resolution STM image for the completely covered Sn films exhibits a square-like structure. The LEED pattern shows two different primitive spots of Sn film and Al(111), which are shown as yellow and red lines, respectively. The unit cell of ("2"×√3) is also shown as white dotted line.

Fig. 4(a) shows the Sn atomic arrangement estimated from the LEED pattern and STM image for Sn/Al(111). The atomic arrangement can be explained by expanding an ideal hexagonal lattice toward the [-110] direction by approximately 1.5 times, resulting in a square-like unit cell, which are shown as yellow line. Since the square-like unit cell is incommensurate, the unit cell of ("2"×√3) is used in this study. The atomic arrangement of the monolayer Sn film is very similar to the Sn film on Rh(111) and Ru(0001), as shown in Fig. 4(b) and 4(c) [5,6]. The interatomic distance of Sn atoms is close to 0.32 nm.

Fig. 5 shows typical LEED patterns of an atomic layer Pb film before and after Sn deposition up to 0.5 ML. As increasing the amount of Sn deposited onto the (√31×√31)-Pb surface, the LEED pattern gradually changed from (√31×√31) into ("2"×√3). When the total coverage of Pb and Sn is below the saturation coverage (0.65 ML) for single

atomic layer, weak (√31×√31) spots are observed, as shown in Fig. 5(b). Therefore, some Sn atoms deposited are located at the (√31×√31) domains. When the total coverage is above the saturation coverage, the ("2"×√3) patterns are observed, as shown in Fig. 5(c) and (d). Therefore, Most of the Pb atoms forming (√31×√31) structure give their spaces for Sn atoms forming the ("2"×√3)-Sn structure. From the STM image (not shown here), 3D islands at the step edge were newly observed after Sn deposition. While Pb atoms grow layer by layer on Al(111), Pb atoms may form 3D islands on Sn/Al(111). When the Pb atoms are deposited on unsaturated atomic layer of Sn film, the LEED pattern changed from (1×1) into ("2"×√3)-Sn. The result indicates that Pb atoms contribute to saturate the Al(111) surface with Sn and Pb atoms, so that Sn atoms form the ("2"×√3)-Sn structure. In both cases of deposition processes, Pb atoms give a space for Sn atoms on Al(111) and they form a 3D island. From these results, it is concluded that Sn atoms preferentially occupy the surface forming a 2D film and that Pb atoms are located in an uncovered area of the surface or forming 3D island.

Bimetallic films of Pb-Sn were systematically examined to identify their 2D phase diagram on Al(111). Fig. 6 summarize a 2D phase diagram of (Pb,Sn)/Al(111), together with the single element phases for Pb/Al(111) and Sn/Al(111). It should be noted that these phases are not equilibrium since Pb and Sn atoms are deposited at room temperature. At any compositional ratio, LEED patterns only exhibit (√31×√31)-Pb and/or ("2"×√3)-Sn spots in addition to primitive (1×1) spots. No new LEED patterns were observed, regardless of the order of Pb and Sn depositions. Therefore, it is concluded that Pb and Sn are immiscible on Al(111). This is in agreement with the characteristics of the bulk Pb-Sn alloy, but the present result is very different from 2D films of Pb and Sn on Rh(111), Ru(0001), and Ag(111). The high exchange mobility of Sn or Pb at the Pb-Sn film on Al(111) is essential to form two separated phases of

(√31×√31)-Pb and (“2”×√3)-Sn. In other words, the ordered alloy of Pb and Sn obtained on Rh(111) and Ru(0001) may be due to the restriction of surface diffusion of Pb and Sn atoms. On the contrary, in the case of Pb on Si(111), when the Pb metallic layers were formed, unexpectedly high island growth rates, in other word, unusual high collective mobilities of Pb are observed [16]. Therefore, the surface diffusion of Pb is strongly depend on the substrate element in the submonolayer films.

IV. Summary

Binary 2D films of Pb and Sn on Al(111) were studied using STM, LEED, and AES. Pb atoms form a hexagonal close-packed structure and Sn atoms are found to form square-like structure. Although the Pb or Sn structures that formed on Al(111) are similar to those that formed on Rh(111) and Ru(0001), bimetallic Pb-Sn films do not form an ordered alloy; instead, they are immiscible on Al(111).

ACKNOWLEDGMENTS

This work was partially supported by Grants-in-Aid for Scientific Research (C) (Grant No. 26390065) from the Japan Society for the Promotion of Science (JSPS).

REFERENCES

[1] K. Takeda and K. Shiraishi, Theoretical possibility of stage corrugation in Si and Ge analogs of graphite, Phys. Rev. B **50** (1994) 14916.

[2] P. Vogt, P. De Padova, C. Quaresima, J. Avila, E. Frantzeskakis, M. C. Asensio, A. Resta, B. Ealet, G. Le Lay, Silicene: Compelling Experimental Evidence for Graphenelike Two-Dimensional Silicon, Phys. Rev. Lett. **108** (2012) 155501.

[3] M.E. Dávila, L. Xian, S. Cahangirov, A. Rubio and G. Le Lay, Germanene: a novel two-dimensional germanium allotrope akin to graphene and silicene, New J. Phys. **16** (2014) 095002.

[4] Feng-feng Zhu, Wei-jiong Chen, Yong Xu, Chun-lei Gao, Dan-dan Guan, Can-hua Liu, Dong Qian, Shou-Cheng Zhang, and Jin-feng Jia, Epitaxial growth of two-dimensional stanene, Nature Materials **14** (2015) 1020-1025.

[5] J. Yuhara, M. Schmid, P. Varga, Two-dimensional alloy of immiscible metals: Single and binary monolayer films of Pb and Sn on Rh(111), Phys. Rev. B **67** (2003) 195407.

[6] J. Yuhara, Y. Ishikawa, T. Matsui, Two-dimensional alloy of immiscible Pb and Sn atoms on Ru(0001), Surf. Sci. **616** (2013) 131-136.

[7] C.R. Ast, D. Pacilé, M. Papagno, T. Gloor, F. Mila, S. Fedrigo, G. Wittich, K. Kern, H. Brune, M. Grioni, Orbital selective overlayer-substrate hybridization in a Pb monolayer on Ag(111), Phys. Rev. B **73** (2006) 245428.

[8] A. Krupski and S. Mroz, LEED investigation of the Pb and Sb ultrathin layers deposited on the Ni(111) face at T=150–900 K, Surf. Rev. and Lett. **10** (2003) 843-848.

[9] K.J. Rawlings, M.J. Gibson, P.J. Dobson, The epitaxial growth of lead and thallium on (111) silver and copper, J. Phys. D: Appl. Phys. **11** (1978) 2059-2070.

[10] J. Yuhara, M. Yokoyama, T. Matsui, Two-dimensional solid solution alloy of Bi-Pb binary films on Rh(111), J. Appl. Phys. **110** (2011) 074314.

[11] W. Hume-Rothery, R.E. Smallman, C.W. Hayworth, The Structure of Metal and Alloys (The Metals and Metallurgy Trust, London, 1969).

[12] M. Yokoyama, W.S. Liang, W. Chen, A.T.S. Wee, T. Matsui, J. Yuhara, Symmetrical transition of an atomic arrangement for two-dimensional Bi films on Rh(111) in the submonolayer regime, Surf. Sci. **605** (2011) 844-847.

[13] J. Yuhara and T. Ako, Two-dimensional Pb–Sn alloy monolayer films on Ag(111), Appl. Surf. Sci. **351** (2015) 83-88.

[14] Y. Fujiwara, N. Matsubara, J. Yuhara, M. Tabuchi, K. Fujita, N. Yamada, Y. Nonogaki, Y. Takeda, K. Morita, Erbium delta-doping to InP by OMVPE, Inst. Phys. Conf. Ser. **145** (1996) 149-154.

[15] Th. Deniozou, J. Ledieu, V. Fournée, D.M. Wu, T.A. Lograsso, H.I. Li, R.D. Diehl, Aperiodic and modulated Pb thin films on fivefold icosahedral Al-Cu-Fe and Al(111): Tailoring the structure of Pb, Phys. Rev. B **79** (2009) 245405.

[16] M. T. Hershberger, M. Hupalo, P. A. Thiel, C. Z. Wang, K. M. Ho, and M. C. Tringides, Nonclassical “Explosive” Nucleation in Pb/Si(111) at Low Temperatures, Phys. Rev. Lett. **113** (2014) 236101.

FIGURE CAPTIONS

Fig. 1 (a) STM image and (b) LEED pattern at the incident electron energy of 78 eV for Pb film on Al(111) at a coverage of 0.9 ML. The first-order Al(111) substrate spots are marked with open circles. The primitive unit cell of Al(111) and Pb(111) are illustrated with red and yellow lines.

Fig. 2 Structural models of 2D Pb films on (a) Al(111), (b) Rh(111), and (c) Ru(0001). The unit cell of Ag(111), Pb primitive cell, and Al(111)($\sqrt{31}\times\sqrt{31}$)R8.95°-Pb are illustrated with a red solid, yellow solid, and white dotted lines.

Fig. 3 (a) STM image and (b) LEED pattern at the incident electron energy of 78 eV for Sn film on Al(111) at a coverage of 0.8 ML. The first-order Al(111) substrate spots are marked with open circles. The inset in (a) shows the high-resolution STM image. The primitive unit cell of Al(111) and Sn square-like lattice are illustrated with red and yellow lines.

Fig. 4 Structural models of 2D Sn films on Rh(111), Ru(0001), and Al(111). The unit cell of ("2"×$\sqrt{3}$) is illustrated with red lines.

Fig. 5 LEED patterns of Pb and Sn on Al(111) examined with 78 eV incident electron energy (a) at a Pb coverage of 0.35 ML : ($\sqrt{31}\times\sqrt{31}$) pattern; (b) at a coverage of 0.35 ML Pb + 0.3 ML Sn : ($\sqrt{31}\times\sqrt{31}$) pattern; (c) at a coverage of 0.35 ML Pb + 0.4 ML Sn : ($\sqrt{31}\times\sqrt{31}$)+("2"×$\sqrt{3}$) pattern; and (d) at a coverage of 0.35 ML Pb + 0.5 ML Sn : ("2"×$\sqrt{3}$) pattern. The first-order Al(111) substrate spots were marked with open yellow circles.

Fig. 6 2D bimetallic phase diagram of (Pb,Sn)/Al(111). The single element phases for Pb/Al(111) and Sn/Al(111) are also shown in horizontal and vertical lines. The dashed line is the atomic layer saturation coverage for the bimetallic films.

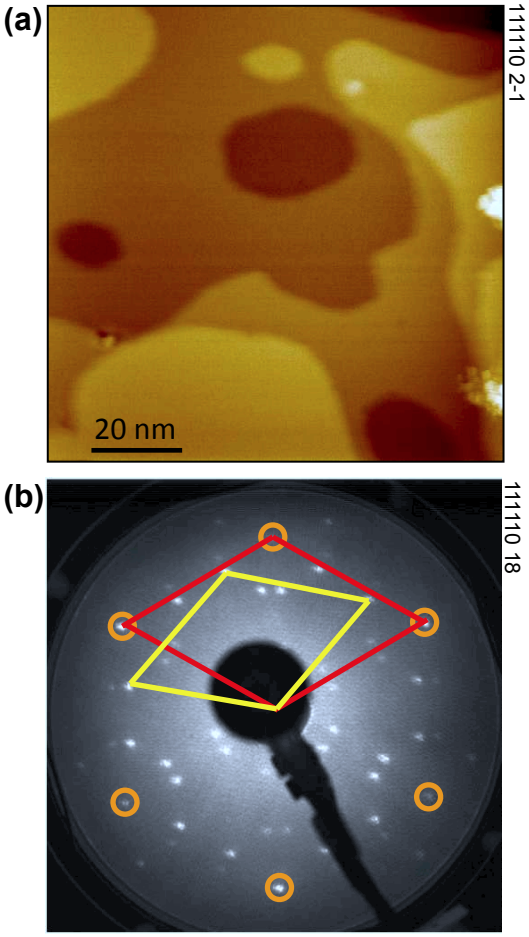

Fig.1

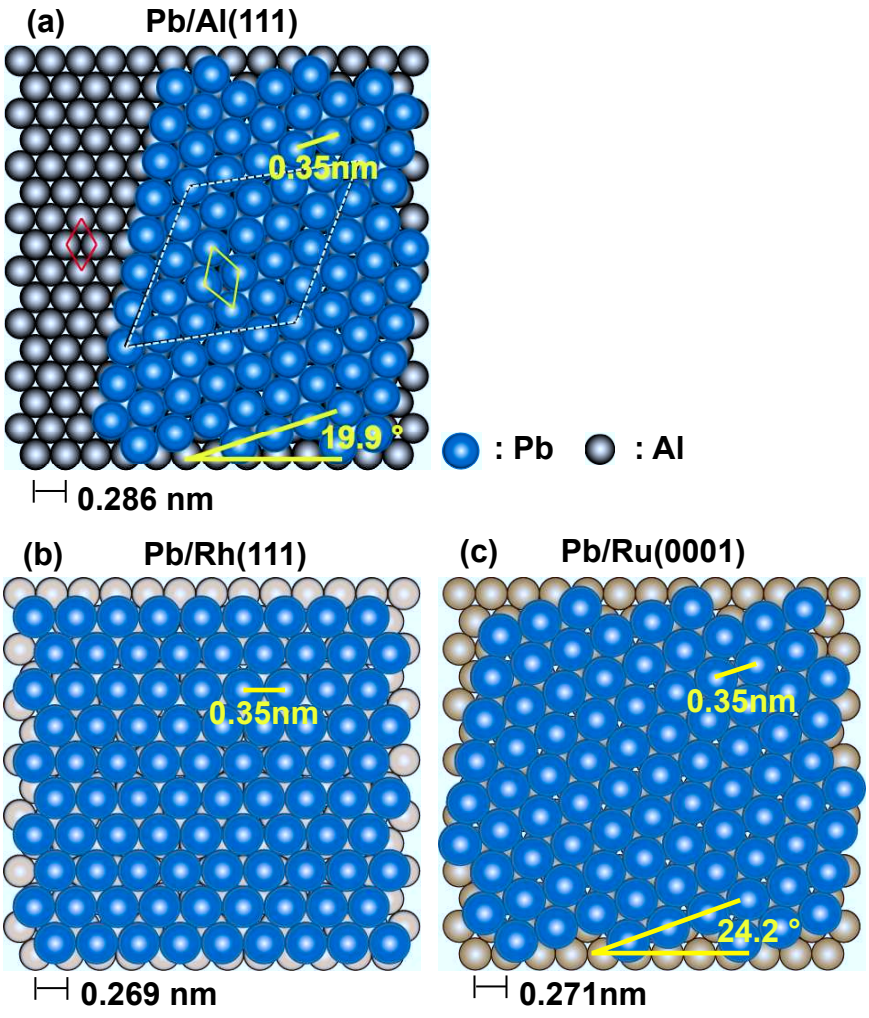
(a) Pb/Al(111)
0.35nm
19.9 °
: Pb
: Al
0.286 nm
(b) Pb/Rh(111)
0.35nm
0.269 nm
(c) Pb/Ru(0001)
0.35nm
24.2 °
0.271nm

Fig.2

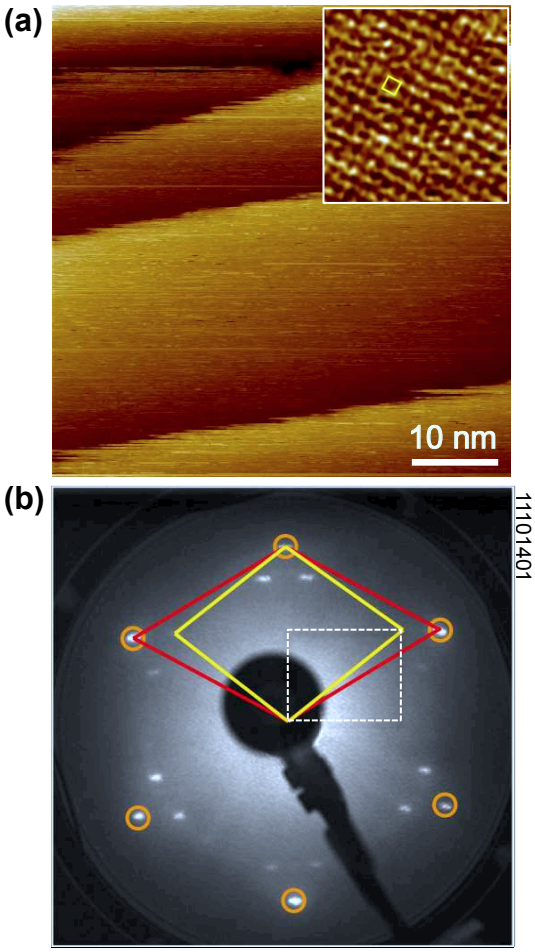

Fig.3

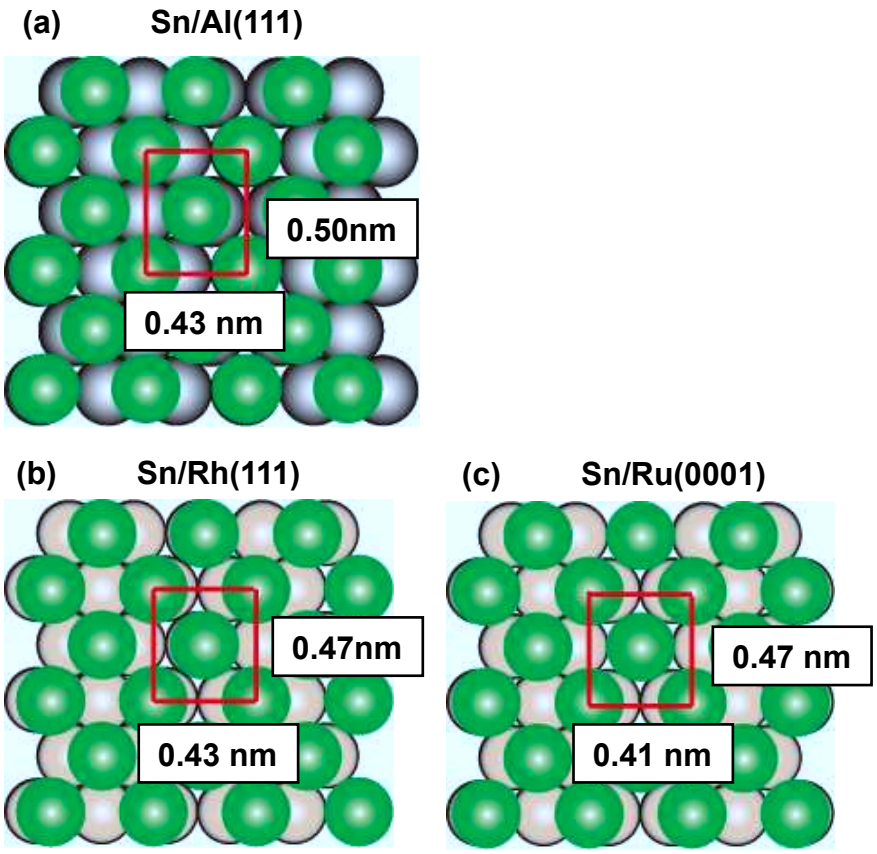
(a) Sn/Al(111)
0.50nm
0.43 nm
(b) Sn/Rh(111)
0.47nm
0.43 nm
(c) Sn/Ru(0001)
0.47 nm
0.41 nm

Fig.4

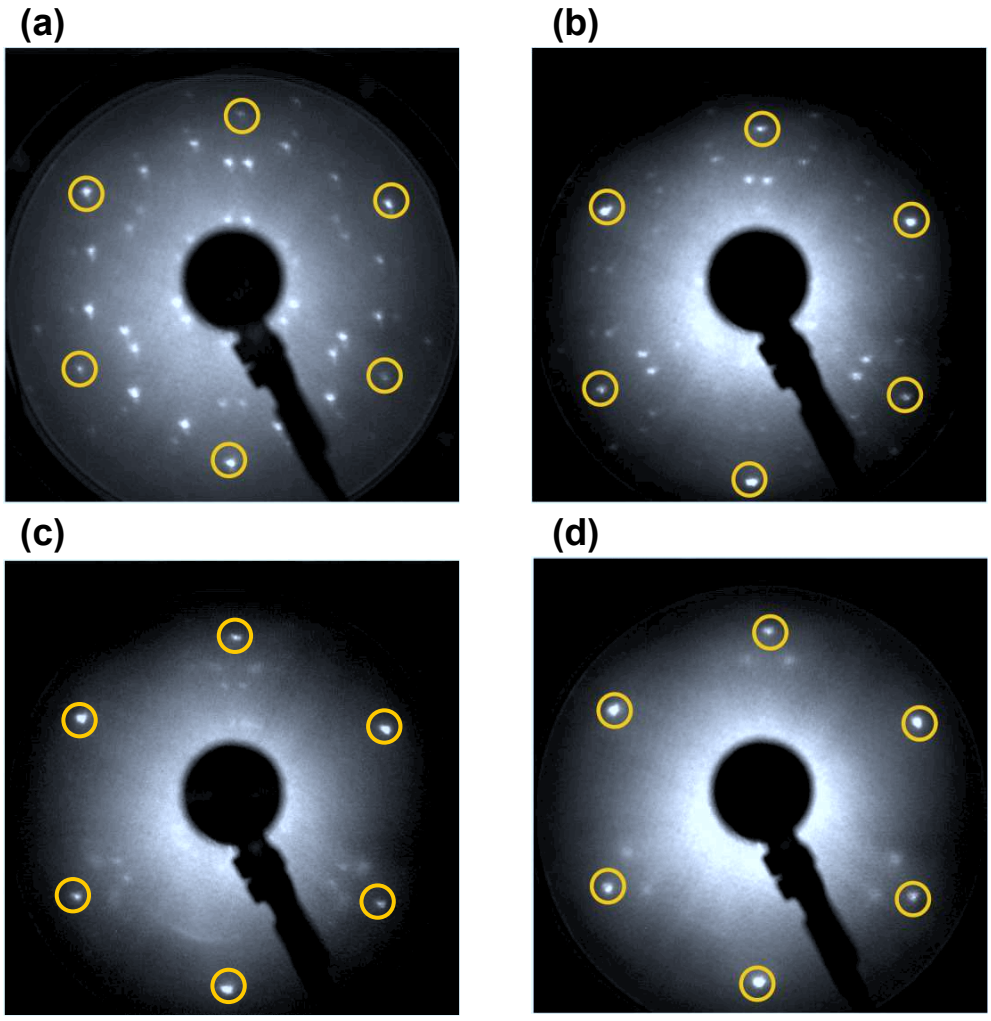

Fig.5

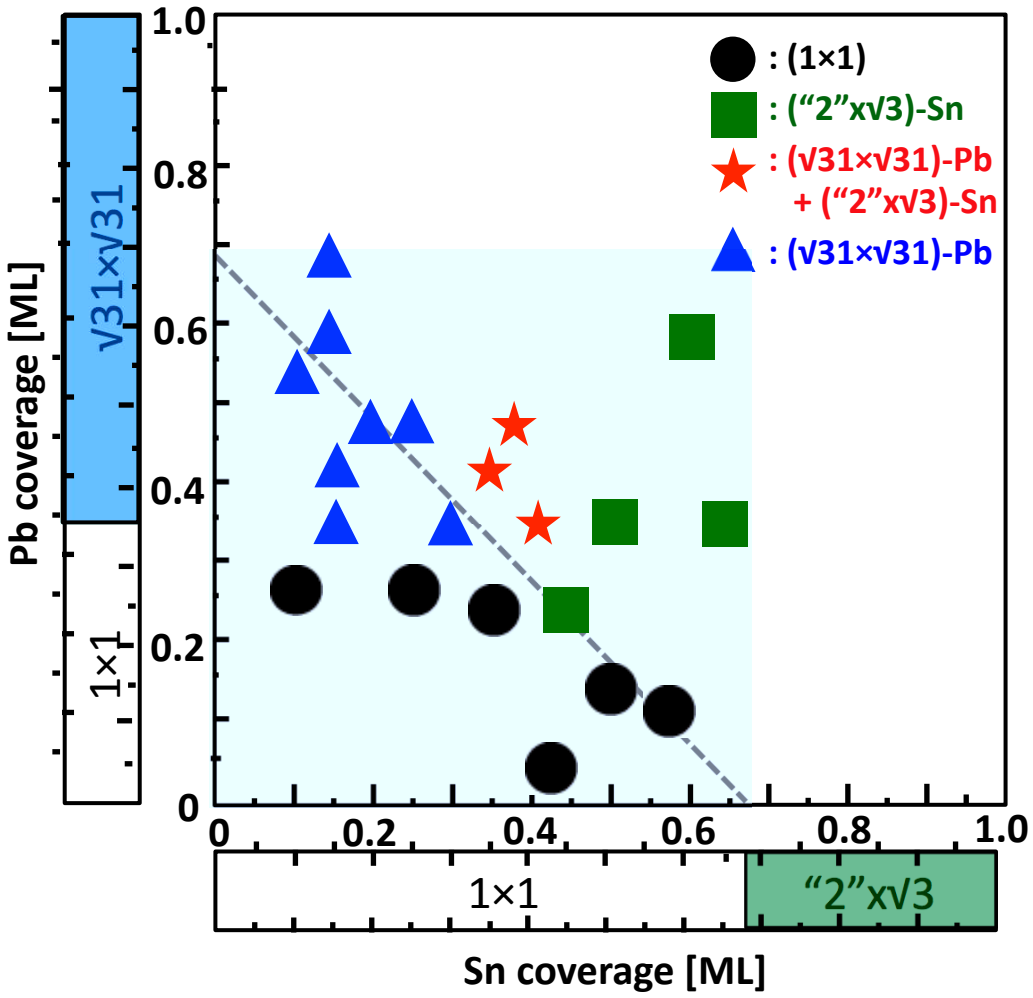
: (1×1)
: (“2”x√3)-Sn
: (√31×√31)-Pb
+ (“2”x√3)-Sn
: (√31×√31)-Pb
Pb coverage [ML]
Sn coverage [ML]
√31x√31
1×1
1×1
“2”x√3
0
0.2
0.4
0.6
0.8
1.0

Fig.6